Fracture Mechanics of Concrete and Concrete Structures -
High Performance, Fiber Reinforced Concrete, Special Loadings and Structural Applications- B. H. Oh, et al. (eds)

Long-term behaviour of cracked SFRC beams exposed to aggressive environment

N. Buratti, C. Mazzotti & M. Savoia
DISTART – Structural engineering, University of Bologna, Bologna, Italy

ABSTRACT: This work describes the first results of an experimental campaign aimed at investigating the long-term behaviour of cracked Steel Fibre Reinforced Concrete (SFRC) beams exposed to an aggressive environment. Initially, the beams were pre-cracked, unloaded and then reloaded for the long-term test with a constant load, in a four-point bending scheme. During the test one of the beams was exposed to drying-wetting cycles of a 5% NaCl solution while the other beam was left unexposed. The long-term test lasted for about 8 months and was performed in a climate-controlled room. The mid-span deflection and the crack opening of the beams were monitored for the entire length of the test. At the end of the long-term test the beams were loaded up to failure. The first results show that the effects of the exposure to the aggressive environment are quite limited on both the long-term behaviour and the ultimate strength.

1 INTRODUCTION

In the last few years the construction industry, supported by the scientific advances and by new standards, has recognized that the concrete pavements have to be designed as structural elements, and must comply with some prescribed limit states (Sorelli et al. 2006). The design of the concrete pavements is mainly addressed by requirements in terms of serviceability limit states (short and long-term deformation, cracking, durability) and only marginally by requirements in terms of ultimate limit states. As far as the serviceability limit states are concerned the performance levels to be satisfied must be defined by taking into account the reference time interval of application of the corresponding actions (characteristic, frequent and persistent values). In order to fulfil these requirements, in the last years there has been a great deal of technical developments concerning the construction materials, among which Steel Fibre Reinforced Concretes (SFRC) have generated noteworthy advances in the concrete industrial pavements technology (Ahmad et al. 2004, Sorelli et al. 2006, Rouse 2007). As an example, the traditional reinforcement mesh may, in some cases, be reduced or completely removed by using fibre reinforced concretes (Miltenberger 2007). Industrial pavements are the most common example of SFRC elements which may not have traditional reinforcement. In order to satisfy durability requirements the assessment of the pavement performances must be verified also with respect to the long-term actions. In this case, the dependence of strains and crack openings on time must be considered, because of their important consequences on durability (Kwon & Shah 2008).

Shrinkage as well may seriously affect the mechanical behaviour of the concrete industrial pavements, either in case of uniform shrinkage or differential shrinkage (Grzybowski & Shah 1991, Altoubat & Lange 2001, Kwon & Shah 2008). In particular, it can produce a curvature of the pavement portions between the joints and, therefore, can cause cracks at the edges. Even if this is an extremely common type of damage for the concrete industrial pavements, the experimental data on their long-term behaviour are very limited.

The present paper is a first attempt in understanding the long-term behaviour of SFRC elements exposed to aggressive environments, which can be important for pavements not protected from weather. In particular, the present paper discusses the results of tests comparing the long-term behaviour, in terms of deflection and crack opening, of a SFRC beam exposed to drying-wetting cycles in a chloride solution with analogous results for an identical SFRC beam under the same loading conditions but with no aggressive exposition. The beams do not contain any traditional reinforcement. Their geometry (see Section 2) was defined in order to be representative of a strip of industrial pavement.

Other tests are available in the literature (Ferrara et al. 2004, Teruzzi et al. 2004) but the most important aspect of the present work is that the aggressive exposition occurs while the beam is under loading with the cracks wide opened.

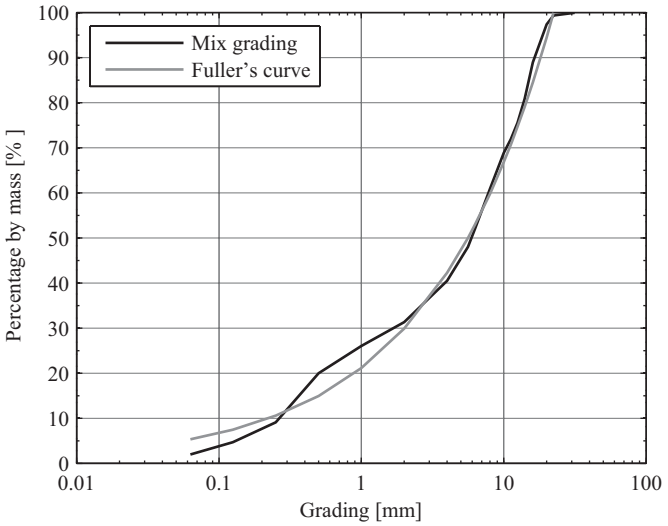

Figure 1. Aggregate grading curve for the concrete mix used in the present study.

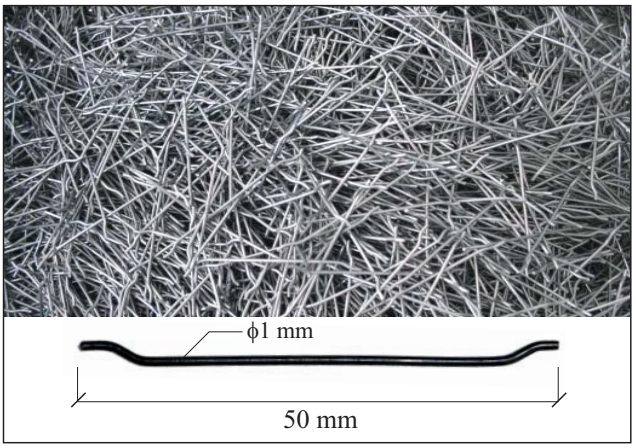

Figure 2. Geometry of the fibres used in the present study.

2 DESCRIPTION OF THE EXPERIMENTAL CAMPAIGN

In the present study, the long-term behaviour of two 2000×300×120 mm^3 (length × width × height) SFRC beams, with no traditional reinforcement, loaded according to the four point bending scheme was investigated. During the long-term test, one of the beams (Beam 2 in the following) was exposed to drying-wetting cycles of a 5% NaCl solution while the other beam (Beam 1) was left unexposed. The dimensions of the beams were chosen in order to be representative of a strip of industrial pavement. This approximation does not take into account the bi-dimensional behaviour of pavements.

In the following section the most important aspects of the experimental campaign are described.

2.1 *Material properties*

The concrete mix used in the present study was defined in order to reach a desired value of the flexural tensile strength, similarly to what is suggested by EN 14845-1. In order to fulfil this requisite some preliminary tests were performed, in which specimens casted using different values of water/cement ratio and different types of aggregates were tested.

This phase of the study led to the definition of the concrete mix which in Table 1. The amount of superplasticizer was adjusted in order to obtain similar slumps in the two casts; 3.5 l/m^3 and 4.2 l/m^3 were used when casting Beam 1 and Beam 2, respectively. Figure 1 shows the aggregate grading.

Table 1. Mix design of the concrete.

Component	Unit	Amount
Cement (CEM I 42.5)	kg/m^3	350.0
Sand (0-5 mm)	kg/m^3	752.4
Gravel (8-15 mm)	kg/m^3	642.3
Gravel (15-22 mm)	kg/m^3	440.4
Water	l/m^3	175.0
Superplasticizer	l/m^3	3.5/4.2

Table 2. Fresh concrete properties.

Code	Slump cm	Hydration temperature °C	Density kg/m^3
Beam 1	16	23.3	2404*
Beam 2	15	23.3	2382*

*with fibres

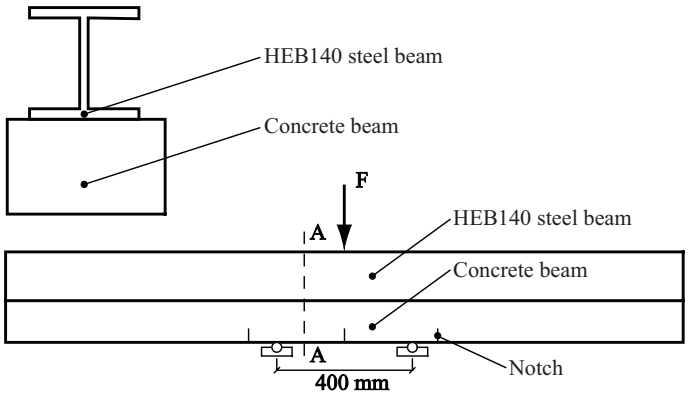

Figure 3. Test set-up used to pre-crack the beams. Three cracks were opened on each beam.

Steel fibres were added to the concrete mix described above; the geometry of the fibres is depicted in Figure 2. According to the producer, these fibres had an elastic modulus of 210 GPa and a tensile strength of 1100 MPa. Both beams were cast with 25 kg/m^3 of fibres.

2.2 *Pre-cracking of beams*

Prior to the long-term tests, the beams were pre-cracked in three cross sections, up to a crack mouth opening displacement (CMOD) of about 0.5 mm. This value was assumed as representative of the upper limit to the crack width of concrete pavements at

the serviceability limit state. In the following, the cracks will be indicated with the letters A, B, and C. In order to better control the position of the crack, the beams were notched (5 mm deep notch). In this phase, a three-point bending scheme was adopted and cracking was done under mid-span displacement control. In order to obtain a more stable fracture process and a better control of the crack width, a HEB140 steel beam was laid upon each concrete beam and connected to it using three separate supports: one at mid-span and two over the external supports of the concrete beam (see Fig. 3). The load was then applied to the steel beam.

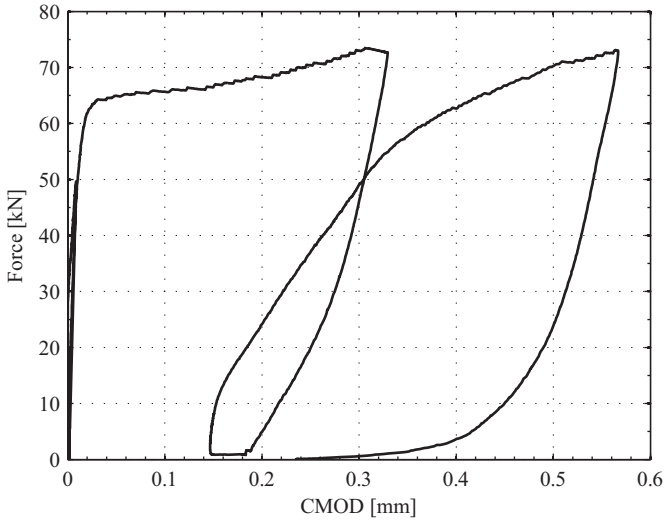

Figure 4. Total force-CMOD curves measured during the opening of crack A on Beam 2 (See Fig. 3 for the test set-up).

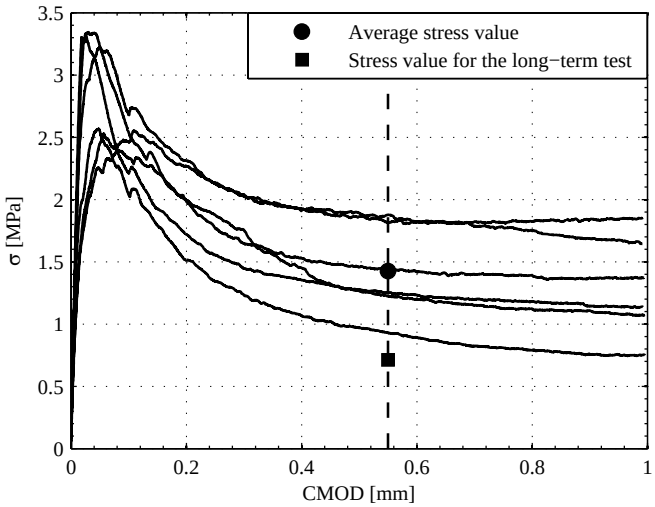

Figure 5. Flexural stress – CMOD curves for the 550×150×150 mm^3 specimens, used to calculate the load to be applied to the beams during the long-term test.

Figure 4 shows the force-CMOD curve recorded while producing one of the cracks on Beam 2. It is important to note that the force measured and reported in the Figure refers to the steel beam - concrete beam system. As a consequence of the experimental set-up adopted it is not possible to separate the behaviour of the SFRC beam form that of the steel beam, unless one uses a theoretical interpretative model.

Figure 6. Experimental setup used for the long-term test. The container used to keep the saline solution can be seen in the centre of the picture.

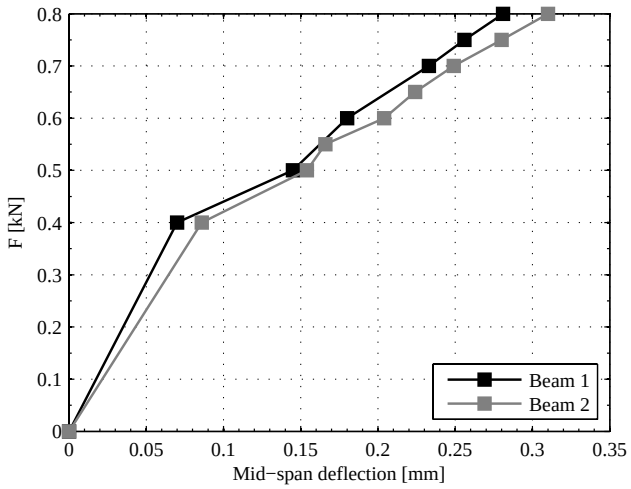

Figure 7. Force - mid-span deflection curve during the loading phase.

Finally, it should be noted that the test was not completely stable and consequently some cracks opened up to 0.5 mm as desired, while others reached 0.6 mm.

2.3 *Determination load for the long-term tests*

In order to define the loading level to be applied during the long-term tests, six 550×150×150 mm^3 (length×width×height) notched prisms, made with the same concrete used for the beams to be tested, were subjected to failure test. According to EN 14651:2005, these tests were performed by using a three-point bending scheme and under crack mouth displacement (CMOD) control; in particular, during the test a prescribed CMOD velocity was followed: 0.05 mm/min for CMOD ≤ 0.1 mm and 0.2 mm/min for CMOD > 0.1 mm The applied force and the corresponding CMOD were measured using a load cell and a displacement transducer, respectively. Figure 5 shows the mid-span flexural stress-CMOD curves of the notched sections, obtained from the tests. The

nominal stress is calculated by dividing the bending moment at mid-span by the elastic section modulus of the notched un-cracked section.

The long-term test performed on Beam 1 and 2 are not standard and there is no code prescribing the load value to be used. In the present work it was chosen to apply, during the long-term tests, the load value giving a nominal stress at the mid-span equal to 50% of the average value of the flexural stresses calculated for the prisms at CMOD = 0.55 mm. This CMOD value corresponds approximately to the crack width produced in the beams in the pre-cracking phase. Obviously, the differences in the loading schemes of the two types of tests must be taken into account. The value 0.80 kN for the force to be applied at the ends of the beams for the long-term test is then obtained (see Fig. 5).

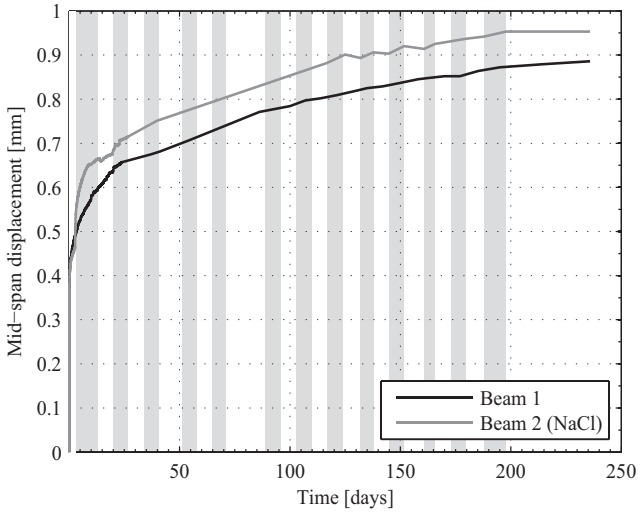

Figure 8. Mid-span displacement increase over time. Shaded zone indicate exposure to the 5% NaCl solution.

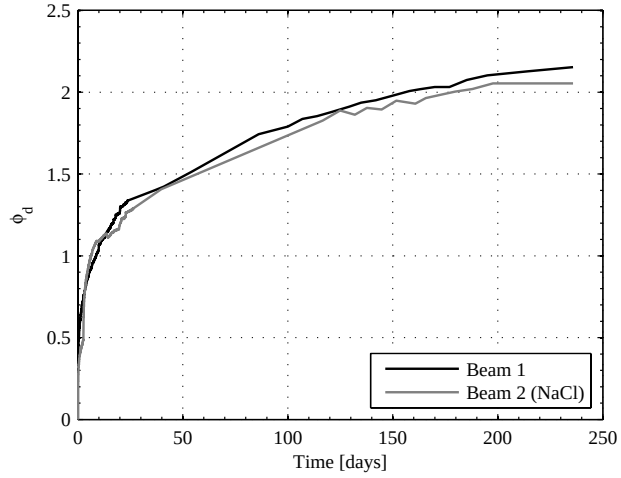

Figure 9. Creep coefficient related with the mid-span displacement.

2.4 *Test procedure*

The two beams were tested adopting a four-point bending scheme. The load was kept constant for 8 months. One of the beams (Beam 2) was subjected, during the long-term test, to drying-wetting cycles of a 5% NaCl solution. Normally, both the wet and the dry phases lasted one week each.

The experimental setup is shown in Figure 6. During the long-term test, each beam was sustained by two steel trestles at the intermediate supports, thus creating a central span of 750 mm with constant bending moment. The dead loads were applied at the beam extremities at a distance of 525 mm from the inner supports. The load was applied by using some steel plates, laid on a steel supporting system composed of a base plate connected by two threaded rods to a transverse hollow rods placed on the upper face of the beam.

On each beam, the crack openings as well as the mid-span deflection with respect to the intermediate supports were measured. The crack opening was measured by using an optical device while the deflection was measured, on both sides of the beams, by using LVDT transducers. In order to measure the relative displacement between mid-span and intermediate supports, two aluminium bars, supported by pins glued over the supports, were placed on both sides of the beams.

During the long-term tests, the beams were kept in a climate room, at 20 °C and RH 60%.

3 RESULTS OF THE LONG-TERM TESTS

In the following section, the results of the long-term tests will be discussed. The results of the failure tests performed at the end of the long-term tests will be discussed as well.

3.1 *Mid-span deflection*

Figure 7 shows the mid-span deflection increase during the loading phase. Each point corresponds to the load given by one of the steel plates used. The number of points on the two curves is not the same because steel plates of different weight were used for the two beams. At the end of the loading phase the two beams showed similar values of mid-span deflection: $\delta_0 = 0.28$ mm for Beam 1 and $\delta_0 = 0.32$ mm for Beam 2. At the end of this loading phase the load was kept constant for 238 days

Figure 8 shows the mid-span deflection evolution with time, for both beams. The shaded zones indicate the periods during which Beam 2 was exposed to the Chloride solution.

After 238 days of loading, the mid-span deflection values measured on Beam 1 and Beam 2 were $\delta_{end} = 0.80$ mm and $\delta_{end} = 0.95$ mm, respectively.

In order to allow a better comparison of the behaviour of the two beams, the creep coefficient, ϕ_d, related with the mid-span displacements was calculated as

$$\phi_d = \frac{\delta(t) - \delta_0}{\delta_0}, \quad (1)$$

where $\delta(t)$ is the mid-span displacement at the general time t and δ_0 is the mid-span displacement at the end of the loading phase (see Fig. 7). Figure 9 shows the curves obtained using Equation (1). Long-term deformation at the end of the test was 2.15 and 2.05 times greater than the initial values for Beam 1 and Beam 2, respectively. Figure 9 makes clear that the curves corresponding to the two beams are very similar and suggest that the effects of the saline solution on mid-span deflection are in this case very small.

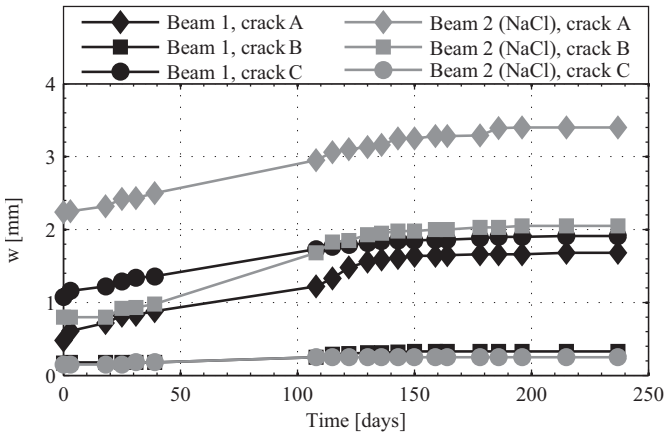

Figure 10. Increase of the crack widths over time.

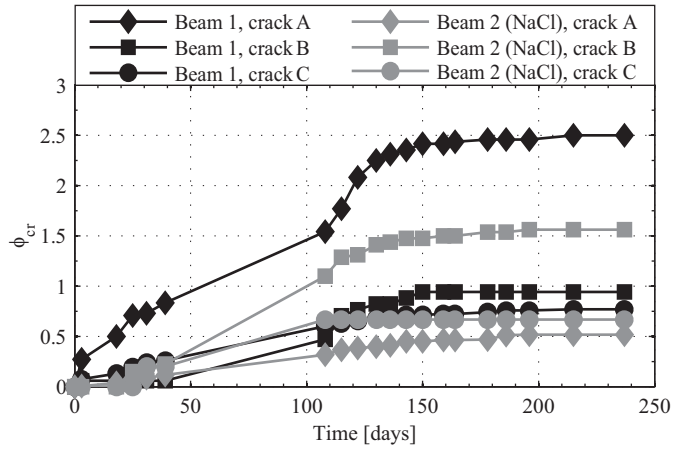

Figure 11. Creep coefficient related with the crack opening.

3.2 *Crack opening*

The crack widths w were measured, using an optical device, in three points for each crack and therefore each measure took a long time. Then, for each crack the average value of the three measures was calculated.

Figure 10 shows the mean values of the crack width increase over time for each one of the three monitored cracks on the two beams. It is important to note that the initial values are very different because the pre-cracking test was not completely stable. It should also be noted that the crack width values given in Figure 10 are quite greater than the CMOD values given in Figure 4, because the reloading of the beams was done up to a load level with is the average of those reached in the cracking phase of the 550×150×150 mm^3. Therefore the widths of the different cracks subjected to the same bending moment are different.

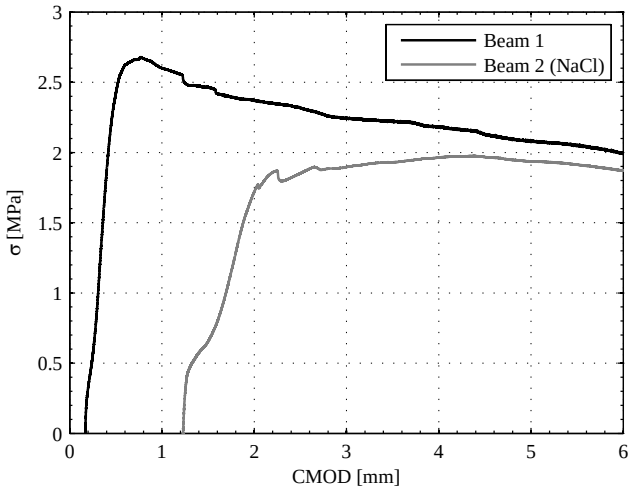

Figure 12. Flexural stress-CMOD curves for the middle crack, measured at the end of the long-term tests.

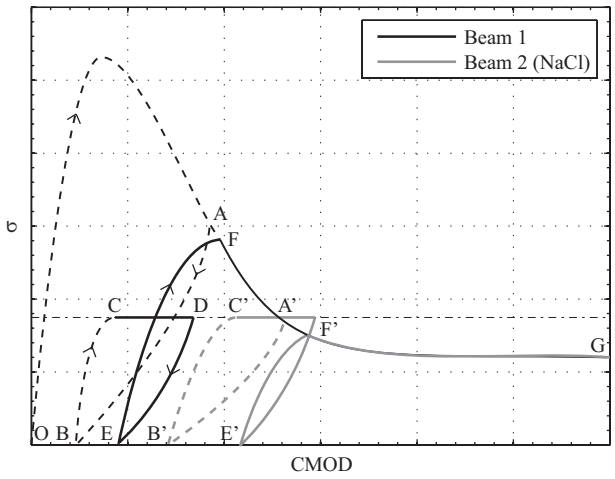

Figure 13. Flexural stress-CMOD curves for the middle crack, measured at the end of the long-term tests.

In order to allow a better comparison, the creep coefficient related with the crack width increments over time were calculated as:

$$\phi_{cr} = \frac{w(t) - w_0}{w_0}, \quad (2)$$

where $w(t)$ is the general crack width at time t and w_0 is the crack width at the end of the loading phase. The relative crack-width increments are plotted in Figure 11. These curves are quite different even for cracks on the same beam. In fact, for the cracks on Beam 1 the crack-width increase at the end of the test ranges from 0.77 to 2.5, with a mean value equal to 1.40, while for Beam 2 it ranges from 0.51 to 1.56, with a mean value equal to 0.91. This Figure

confirms the conclusions taken from the mid-span displacement data; the effects of the exposure to the NaCl solution seem to be negligible (at least for the test duration considered).

3.3 *Failure test*

After 238 days under constant loading the beams were unloaded and reloaded up to failure. The beams were loaded in three-point bending and the load was applied in correspondence of the mid-span crack. The position of the supports was between the centre and the lateral cracks (the distance of the supports was equal to 510 mm) in order to have only one crack in the loaded portion of the beam.

Figure 12 shows the flexural stress-CMOD curves obtained from these tests. It should be noted that the first point of the curves does not coincide with the origin of the axes because the first CMOD value was set equal to the crack width measured at the end of the unloading phase. The different behaviour can be explained by considering the quite different widths of the cracks obtained at the end of the long-term loading-

The loading history of the cracked sections is shown schematically in Figure 13, considering a theoretical stress-CMOD curve for the fibre reinforced concrete beams. With reference to Beam 1, O-A-B indicates the pre-cracking test, B-C indicates increase of crack width during the long-term test, C-D the creep deformations occurred during the long-term tests, D-E the unloading phase and E-F-G the failure test. The points characterising the load history for Beam 2 are indicated with the same letters denoted by an apostrophe. The different behaviour that the two beams show in Figure 12 may therefore be explained by considering that the crack opening for Beam 2 is greater than for Beam 1 and therefore, as illustrated in Figure 13, during reloading Beam 2 (E'-F'-G) may reach directly the sub-horizontal branch of the theoretical curve representing the monotonic loading. Hence, it can be concluded that the curves in Figure 12 may confirm the conclusions on the negligibility of the effects of the exposure to the chloride solution which were drawn from mid-span deflection and crack-width increases over time in the long-term test.

4 CONCLUSIONS

In the present work, the durability of steel fibre-reinforced concrete beams was investigated and in particular the effects of the exposure to a chloride solution.

Two cracked beams were tested for about 8 months under constant loading and one of them was exposed to drying-wetting cycles of a 5% NaCl solution. For the entire duration of the test the crack width and the mid-span deflection of the beams were measured.

At the end of this phase the beams were unloaded and taken for a failure test.

Even if this is a preliminary study, and the number of specimens considered is extremely small, the tests performed suggest that the effects of the exposure to the chloride solution are very limited. Both the long-term behaviour and the residual strength of the steel fibre reinforced concrete beams did not show any significant change due to the aggressive environment.

5 ACKNOWLEDGEMENTS

The financial support of Maccaferri Group is gratefully acknowledged.

REFERENCES

Ahmad, A. Di Prisco, M. Meyer, C. Plizzari, G.A. & Shah, S.P. 2004. *Fiber reinforced concrete: from theory to practice*, 24 - 25 September, Bergamo, Italy.

Altoubat, S.A. & Lange, D.A. 2001. Creep, shrinkage, and cracking of restrained concrete at early age. *ACI Materials Journal* 98(4): 323-331.

EN 14651:2005 2005. *Test method for metallic fibered concrete - Measuring the flexural tensile strength (limit of proportionality (LOP), residual).*

EN 14845:2006 2006. *Test methods for fibres in concrete*.

Ferrara, L. Fratesi, R. Signorini, S. & Sonzogni, F. 2004. Durability of steel fibre-reinforced concrete precast elements: experiments and proposal of design recommendations. *6th RILEM Symposium on Fibre-Reinforced Concretes (FRC) – BEFIB 2004.* 20-22 September, Varenna, Italy.

Grzybowski, M. & Shah, S.P. 1990. Shrinkage cracking of fiber reinforced conrete. ACI Materials Journal. 87(2): 138-148.

Kwon, S.H. & Shah, S.P. 2008. Prediction of early-age cracking of fiber-reinforced concrete due to restrained shrinkage. *ACI Materials Journal* 105(4): 381-389.

Miltenberger, M. Attiogbe, E. & Bissonnette, B. 2007. Behavior of conventional reinforcement and a steel-polypropylene fiber blend in slabs-on-grade. *Materials and Structures* 40(3): 279-288.

Rouse, J.M. & Billington, S.L. 2007. Creep and shrinkage of high-performance fiber-reinforced cementitious composites. *ACI Materials Journal* 104(2): 129-136.

Sorelli, L.G. Meda, A. & Plizzari, G.A. 2006. Steel fiber concrete slabs on ground: a structural matter. *ACI Structural Journal* 103(4): 551-558.

Teruzzi, T. Cadoni, E. Frigeri, G. Cangiano, S. & Plizzari, G.A 2004. Durability aspects of steel fibre reinforced concrete. *6th RILEM Symposium on Fibre-Reinforced Concretes (FRC) – BEFIB 2004.* 20-22 September, Varenna, Italy.